

Chemical weathering in a region of active orogeny: Pescadero Creek Watershed, California

R. D. Phillips and S. Rojstaczer

Division of Earth and Ocean Sciences and Center for Hydrologic Science, Duke University, Durham

Abstract. Base flow chemical signals were used to determine the weathering reactions that control the groundwater chemistry of a geologically heterogeneous, mountainous watershed. Major ion signatures result from cyclic salt and formation water inputs and from the weathering of easily oxidized or highly soluble minerals, such as pyrite, calcite, and dolomite. If montmorillonite is the dominant secondary mineral product, then the bulk of silicate weathering probably involves volcanic rocks. Spatial rates of base flow chemical denudation range from 0.0004 to 0.02 mm yr⁻¹, and temporal rates range from 0.0006 to 0.6 mm yr⁻¹. The mean chemical denudation rate for the watershed is 0.03 mm yr⁻¹, which is comparable to some of the world's most rapidly weathering large drainage basins. Because highly soluble or easily oxidized minerals contribute the bulk of the chemical signal to basin waters, spatial and temporal rates of chemical denudation are constrained largely by recharge and discharge rather than local variations in lithology.

1. Introduction

Solute discharges of the world's major rivers indicate that areas of active orogeny tend to have elevated chemical-weathering rates relative to the rest of the Earth's surface [Summerfield and Hulton, 1994]. The implications of silicate weathering in these regimes on the global CO₂ budget and climate are potentially very significant [e.g., Volk, 1993; Moore and Worsley, 1994].

It is, however, difficult to quantify the influence of tectonic uplift upon weathering through the use of field measurements. Measurements of mass flux from tectonically active watersheds in conjunction with geochemical modeling may allow for such analysis. However, hydrogeochemical investigations in tectonically active, mountainous watersheds are often complicated by extreme geologic heterogeneity and coastal settings. In these watersheds, groundwaters may acquire chemical signals from diverse lithologies, formation waters, and atmospherically deposited cyclic salts. Consequently, extensive spatial sampling is required to characterize the processes by which the groundwaters obtain their chemical signatures.

Measurements of chemical denudation generally have been confined to large-scale watersheds, and there is little information on fine-scale variability in denudation rates. In this study, we use base flow chemical signals to determine the weathering reactions that control groundwater chemistry in a coastal central California watershed (Pescadero Creek) and use chemical and discharge data to calculate spatial and temporal rates of chemical denudation. The Pescadero Creek watershed is located in a region of active tectonic uplift [Anderson and Menking, 1994], and the Mediterranean climate of the area aids in the spatial sampling of basin groundwaters. Virtually no precipitation falls during the summer months, so streams are dominated by base flow conditions and are essentially an integrated surface expression of the groundwater at any point in the system. Our measurements are used in conjunction with previous seasonal measurements of water quality [Baldwin, 1967a, 1967b; Steele,

1968] in the watershed. In this region, silicate weathering apparently is only a minor contributor relative to chemical denudation caused by carbonate and possibly pyrite dissolution. Rates of denudation are comparable to those estimated for the major active continental mountain belts in the world.

2. Study Area

2.1. Geography

The Pescadero Creek watershed is located in the Santa Cruz Mountains of California between latitudes 37°11'30"N and 37°19'N and between longitudes 122°7'30"W and 122°24'30"W (Figure 1). The watershed encompasses a total area of 211.6 km², and elevation ranges from sea level to 820 m. The topography of the eastern portion of the basin is dominated by the rugged, irregular relief of the Santa Cruz Mountains and yields westward to the flat marine terraces of the coastal regions [Baldwin, 1967b]. Owing to its relatively low human population, anthropogenic effects on the watershed appear to be minimal.

Annual precipitation ranges from 50 cm at the coast to 140 cm at the ridges of the Santa Cruz Mountains [California Department of Water Resources, 1966]. Approximately 90% of the annual precipitation falls between the months of November and April [Steele, 1968] as frequent storms move inland from the northern Pacific.

2.2. Geologic Setting

The geology of the Pescadero basin has been well documented by Cummings *et al.* [1962], Nilsen and Brabb [1979], Clark [1981], Brabb and Pampeyan [1983], and Brabb [1989] among others. The lithology of the Pescadero Creek watershed consists mainly of a thick sequence of Tertiary marine clastic sedimentary rocks (Figure 2). Some carbonate and volcanic rocks are interspersed among the marine sandstones, mudstones, and shales and assorted Quaternary deposits that overlie the Tertiary strata. The entire sequence is underlain by crystalline basement [Clark, 1981]. The sedimentary marine units commonly contain formation water pockets that cause ion concen-

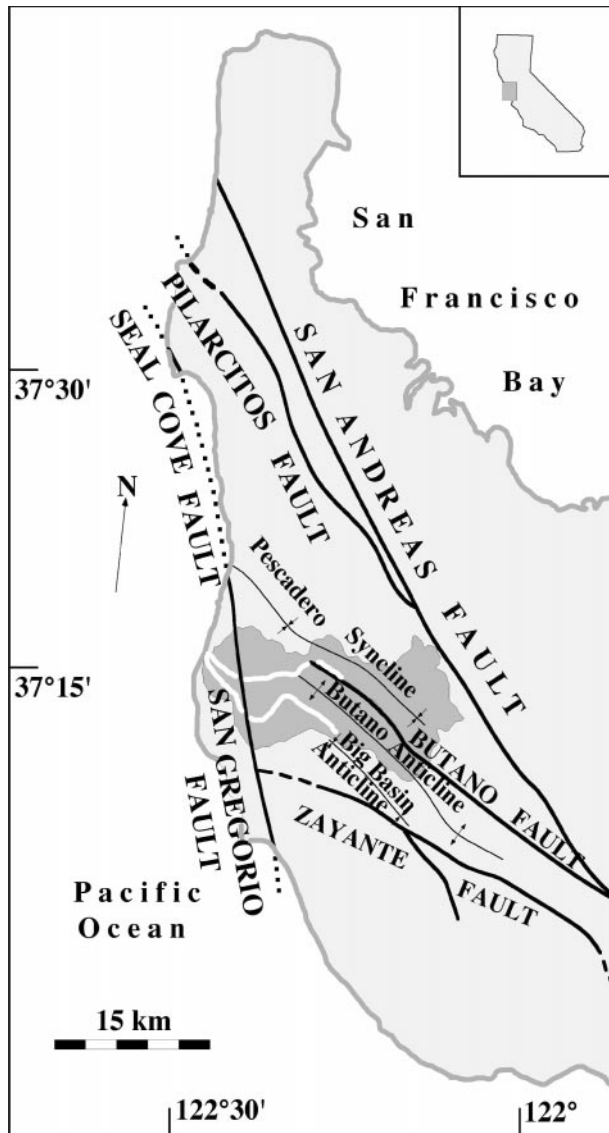


Figure 1. Location and geologic setting of the Pescadero Creek watershed (adapted from *Nilsen and Brabb [1979]*).

tration to increase with depth, especially in the lower Tertiary units such as the Butano Sandstone and the San Lorenzo Formation [*Johnson, 1980*]. Formation water persists in the system because it tends to stagnate in synclinal axes where it cannot be flushed by fresh groundwater [*Akers and Jackson, 1977*].

Because of the complex geology, it is difficult, if not impossible, to quantify mineralogy on a basin-wide scale. Common primary silicate minerals include quartz, micas, and potassium, sodium, and calcium feldspars. Dolomite, calcite, gypsum, anhydrite, halite, and pyrite are also common [*Clark, 1981*].

Uplift rates of marine terraces in the Santa Cruz Mountains are estimated to be 0.9–1.6 mm/yr [*Anderson and Menking, 1994*]. The Pescadero basin is cut by a number of active faults, including the north-south trending San Gregorio fault in the western part of the basin and the east-west trending Butano fault in the eastern part of the basin.

3. Methods

3.1. Field Methods

Field samples and measurements were taken in June and July of 1992 and 1993. Base flow samples were collected for analysis of major chemical constituents and were filtered through 0.45 μm Gelman Supor-450 membrane filters into polyethylene bottles. Filters were flushed with 300 mL of sample water before each sample was bottled. Samples to be analyzed for cations were acidified to a pH of 2 using concentrated nitric acid, and samples to be analyzed for anions and silica were left unacidified. At each sample location (Figure 3), measurements of temperature, pH, specific conductivity, and salinity were taken directly from stream waters. Discharge was also measured at each sample location, using a current meter and calibrated rod. However, given the difficulty of measuring the low discharge of the rocky-channeled streams, the discharge data are assumed to be accurate within only 10%.

3.2. Laboratory Methods

Water samples collected in the field, as well as stream and well samples collected in the summer of 1992, were subsequently analyzed for major chemical constituents. Major cations were determined by DCP spectrometry, and major anions were determined by ion chromatography. Carbonate alkalinity was determined by titration and Gran evaluation as described by *Gieskes and Rogers [1973]*. Silica concentrations were determined colorimetrically using a Gilford spectrophotometer.

The 1992 base flow samples had a mean charge balance error of -0.9% with a standard deviation of 4.6%, and the 1993 base flow samples had a mean charge balance error of 1.5% with a standard deviation of 3.8% (Table 1). Analytic precision was better than 5% in the determination of all chemical constituents.

3.3. Cyclic Salt Corrections

The importance of atmospheric deposition to river-dissolved load has been documented in numerous studies, including investigations in the Pescadero basin by *Baldwin [1967b]* and *Steele [1968]*. *Steele [1968]* collected and analyzed bulk precipitation during the rainy season of 1966–1967 and estimated that atmospheric wet deposition accounted for 25% of the Cl^- transported by Pescadero Creek at the United States Geological Survey (USGS) gauging station. However, this estimate ignored the significant contribution of dry particulates and fog during the summer months. *Baldwin [1967a]* indirectly calculated that the combination of atmospheric wet and dry deposition made up 35% of the Cl^- transported by Pescadero Creek at the gauging station. Two high-elevation base flow samples collected in this study have Cl^- concentrations which are 31 and 34%, respectively, of the base flow Cl^- concentration measured at the USGS gauging station. These samples, collected at the headwaters of Peters Creek and Lambert Creek (Figure 3), are probably representative of the recharge Cl^- composition because they likely have shallow transport paths that have been well flushed of additional Cl^- sources.

Because *Baldwin* based his calculation on data collected at the USGS gauging station, his figure may underestimate the atmospheric contribution of Cl^- to the coastal tributaries owing to the preferential settling of heavier marine aerosols closer to the ocean. However, given the available data, the cyclic Cl^- component of base flow was assumed to be 31% of observed base flow signals and was subtracted accordingly. The remaining cyclic ions were subtracted based on their molar ratios to Cl^- . The molar ratios were taken from *Knops [1994]*, who measured wet and dry atmospheric deposition at the Hastings Natural History Reservation, a site

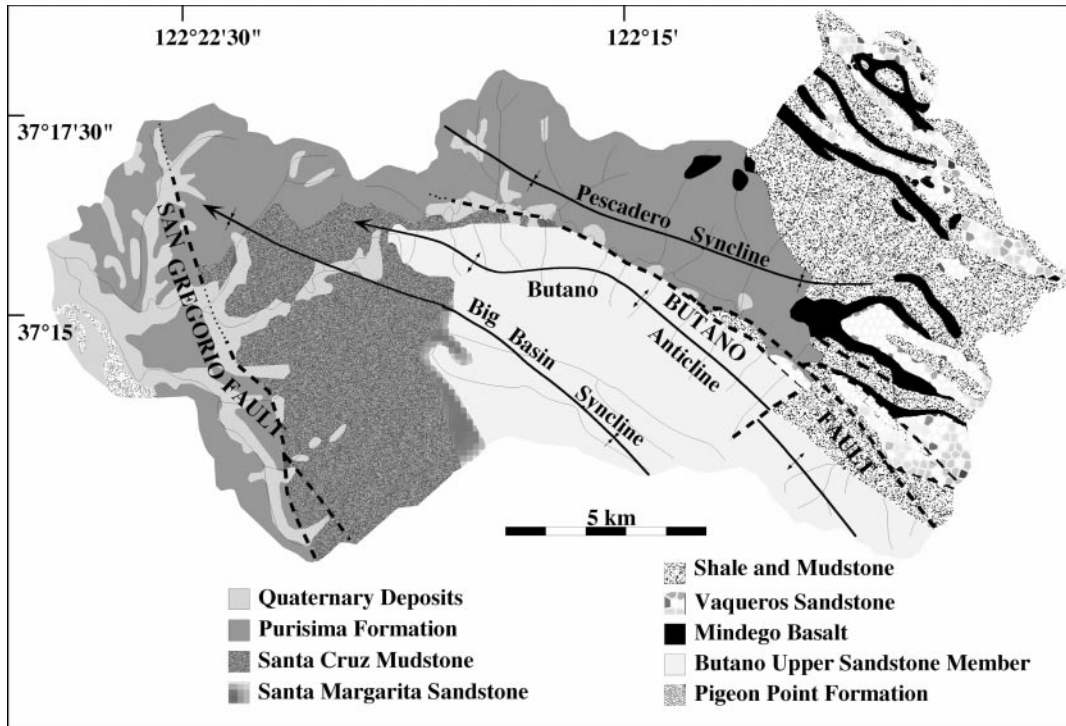


Figure 2. Geologic map of the Pescadero Creek watershed (adapted from *Brabb and Pampeyan* [1983] and *Brabb* [1989]).

located 110 km southeast of the Pescadero basin but with very similar geographic characteristics.

4. Results

4.1. Geochemistry of Basin Waters

The base flow chemical data from 1992 and 1993 are shown in Figure 4. Despite the extreme lithologic variability of the basin, nearly all samples fall in the calcium-bicarbonate field. The lack of compositional variation suggests that the waters of the Pescadero basin receive their respective signals from the same suite of weathering reactions. Of the possible mineral sources, calcite, dolomite, and pyrite are the most ubiquitous and easily weathered [Clark, 1981]. However, saline formation waters are also found throughout the sedimentary units of the basin [Johnson, 1980] and appear to mix with groundwaters and contribute a significant portion of the chemical signal to discharge Baldwin, 1967a; Steele, 1968].

If weathering reactions involving carbonate and sulfide minerals and formation water inputs account for the observed chemical signals, then definite stoichiometric relationships between the ions should be present. If saline formation waters are indeed responsible for the observed Na^+ and Cl^- signatures, a 1:1 stoichiometric relationship should be present between $(\text{Na}^+ + \text{K}^+)$ and Cl^- , assuming K^+ also has a sea-salt origin [Stallard and Edmond, 1983]. Figure 5 shows that the data parallel the 1:1 trend but show a slight offset because of excess cations. The excess cations are probably due to the weathering of Na- and K-aluminosilicates prevalent in the clastic sedimentary rocks in the basin [Stallard and Edmond, 1983; Clark, 1981]. Similarly, weathering reactions involving calcite, dolomite, and pyrite should produce a 1:1 stoichiometric balance between the equivalents of $(\text{Ca}^{2+} + \text{Mg}^{2+})$ and $(\text{HCO}_3^- + \text{SO}_4^{2-})$ [Stallard and Edmond, 1983]. Figure 6 shows that the data very closely

approximate this 1:1 trend. Data points that fall below the trend line reflect the presence of excess anions, which are necessary to balance the excess cations derived from the weathering of the aforementioned Na- and K-aluminosilicates [Stallard and Edmond, 1983].

The importance of weathering reactions involving carbonates and sulfides is further exemplified by a ternary plot of the equivalent proportions of $\text{Ca}^{2+} + \text{Mg}^{2+}$, HCO_3^- , and SO_4^{2-} present in the sample waters. Figure 7 shows that within the bounds of analytic precision, base flow samples generally plot within the field expected for a weathering regime dominated by carbonates and sulfides. Contributions of Ca^{2+} and Mg^{2+} from silicate mineral weathering would also fall in this field, but it is not possible to distinguish from stream chemistry alone the weathering reactions producing these ions [Stallard and Edmond, 1983]. Because contributions of Ca^{2+} and Mg^{2+} from silicate weathering cannot be theoretically differentiated from those of carbonate and sulfate weathering, only the silicate weathering reactions involving SiO_2 , Na^+ , and K^+ can be inferred from the chemical data. To determine the Na^+ derived from silicate weathering, the adjusted Cl^- values were subtracted from the adjusted Na^+ values under the assumption that these ions are contributed in equimolar amounts by formation waters.

4.2. Rates of Chemical Weathering and Denudation

Under steady state conditions, the total flux of solutes in the system, Q_t , is given by the following equation:

$$Q_t = Q_r + Q_w + Q_d + Q_g + Q_a + Q_f - Q_p - Q_b,$$

where Q_r is the flux derived from bedrock weathering, Q_w is the flux from atmospheric wet deposition, Q_d is the flux from atmospheric dry deposition, Q_g is the flux from atmospheric CO_2 gas, Q_a is the flux from anthropogenic sources, Q_f is the contribution from formation water, Q_p is the loss of solutes due

Table 1. Chemical and Discharge Data for the Pescadero Creek Watershed

Sample Number	Date Collected	Ca, mg L ⁻¹	Mg, mg L ⁻¹	Na, mg L ⁻¹	K, mg L ⁻¹	Fe, mg L ⁻¹	Mn, mg L ⁻¹	HCO ₃ , mg L ⁻¹	SO ₄ , mg L ⁻¹	Cl, mg L ⁻¹	SiO ₂ , mg L ⁻¹	Discharge, L s ⁻¹
112	June 26, 1992	98.6	20.6	41.5	3.81	0.09	0.01	254.5	114.6	59.5	23.6	1.59
113	June 24, 1992	75.0	17.7	40.0	4.14	0.07	0.00	151.3	153.1	37.5	17.5	1.22
114	June 26, 1992	88.5	19.5	40.8	3.97	0.13	0.01	202.0	142.5	51.8	20.2	1.64
115	June 26, 1992	86.8	14.4	31.3	2.90	0.16	0.02	227.6	72.9	38.5	20.1	0.48
116	June 26, 1992	99.4	22.3	43.5	3.59	0.70	0.30	316.7	78.0	55.1	29.1	2.89
117	June 26, 1992	93.7	20.5	40.0	4.32	0.08	0.15	216.0	80.8	60.1	17.0	1.87
118	June 23, 1992	81.0	14.0	40.0	2.65	0.07	0.01	242.9	118.4	46.5	20.1	2.38
119	June 27, 1992	88.1	19.1	41.0	3.62	0.08	0.02	278.3	87.0	46.6	23.0	32.00
120	June 27, 1992	101.7	26.2	48.8	6.47	0.17	0.01	364.9	111.0	56.4	29.6	15.80
121	June 27, 1992	54.0	35.4	59.4	18.01	0.18	0.00	404.0	45.4	163.7	43.5	0.82
122	June 27, 1992	88.0	21.1	44.6	5.01	0.18	0.01	303.3	90.2	47.9	24.4	46.38
123	June 27, 1992	49.8	30.9	56.1	11.17	0.16	0.06	331.9	66.8	74.9	49.7	0.99
124	June 27, 1992	86.7	21.3	46.5	5.44	0.16	0.01	303.3	89.2	58.8	24.5	48.79
127	June 29, 1992	51.5	30.2	55.5	10.23	0.11	0.01	229.4	129.6	71.3	54.6	0.91
128	June 29, 1992	68.7	42.7	50.0	10.66	0.16	0.09	256.9	167.5	47.4	50.6	0.74
129	June 29, 1992	85.9	22.5	47.8	5.76	0.11	0.00	301.4	92.4	63.7	24.8	78.92
130	June 29, 1992	61.6	37.9	54.0	10.35	0.10	0.01	245.3	157.3	68.4	47.9	2.27
143	July 6, 1992	90.4	18.2	33.8	2.32	0.08	0.00	353.3	61.0	23.2	25.2	20.27
144	July 6, 1992	82.2	18.6	40.1	3.93	0.20	0.06	223.3	108.6	49.1	17.7	10.31
145	July 6, 1992	93.2	23.4	37.1	4.14	0.08	0.01	360.0	82.9	24.5	28.5	3.03
146	July 6, 1992	83.8	17.7	36.8	3.02	0.20	0.04	283.1	78.7	36.0	21.9	31.86
147	July 6, 1992	51.1	31.9	54.2	15.22	0.16	0.03	339.9	127.2	30.9	48.9	0.85
148	July 6, 1992	108.6	25.8	47.2	4.71	0.12	0.02	367.3	103.0	56.6	26.1	10.51
149	July 7, 1992	82.1	23.8	50.8	5.84	0.26	0.09	305.7	98.5	71.2	25.5	59.81
150	July 7, 1992	67.3	19.5	37.0	3.39	0.20	0.03	228.8	70.4	57.0	*	0.57
151	July 7, 1992	79.2	21.7	46.5	5.56	0.12	0.02	291.7	90.8	57.2	*	76.03
153	July 12, 1992	153.6	33.7	42.7	3.93	0.11	0.01	311.2	214.8	25.3	*	1.02
154	July 12, 1992	66.9	19.8	37.9	2.98	0.10	0.01	261.2	54.6	46.6	*	6.14
155	July 12, 1992	106.9	24.1	41.0	3.11	0.13	0.01	344.8	122.2	19.6	22.8	2.27
156	July 12, 1992	82.6	21.7	41.8	3.29	0.12	0.02	292.3	100.4	46.9	22.0	12.60
157	July 12, 1992	86.7	15.6	27.4	2.11	0.08	0.01	313.6	52.4	18.2	24.3	13.88
158	July 18, 1992	45.6	18.4	36.6	4.00	0.08	0.01	263.6	38.7	29.7	24.6	1.39
159	July 18, 1992	54.1	16.5	33.7	3.07	0.14	0.04	247.1	52.3	28.7	23.6	1.81
201	July 7, 1993	92.0	21.0	41.3	3.65	0.28	0.05	284.4	86.7	45.3	23.8	133.40
202	July 7, 1993	103.7	24.8	48.5	3.51	0.16	0.02	285.6	101.9	66.3	23.4	2.78
205	July 7, 1993	91.8	21.4	42.5	3.83	0.11	0.01	283.7	90.9	47.8	24.1	107.26
206	July 7, 1993	64.2	18.0	41.1	3.26	0.17	0.04	183.7	78.1	53.5	24.7	6.06
207	July 8, 1993	92.3	18.1	32.3	2.51	0.13	0.03	282.5	79.0	37.2	*	64.53
208	July 8, 1993	47.8	10.3	27.6	1.99	0.01	0.00	145.2	45.8	36.6	20.4	0.22
209	July 8, 1993	46.0	10.2	20.8	2.45	2.12	0.49	123.3	66.2	25.6	21.8	2.10
210	July 8, 1993	98.5	19.5	35.4	2.65	0.12	0.01	271.5	81.8	41.8	22.6	112.59
211	July 9, 1993	45.4	9.4	20.1	2.08	0.08	0.02	131.2	43.5	30.5	22.4	1.50
212	July 9, 1993	98.8	21.2	38.2	3.22	0.15	0.02	270.3	87.3	40.1	22.9	124.42
213	July 9, 1993	99.2	21.4	38.0	3.22	0.17	0.02	288.6	89.7	40.4	23.1	128.67
214	July 9, 1993	26.2	17.1	34.4	4.01	0.45	0.35	195.3	4.4	51.5	*	0.00
215	July 11, 1993	38.5	11.9	29.5	2.30	0.96	0.03	166.0	28.3	37.1	18.8	59.35
216	July 11, 1993	12.2	9.5	37.2	3.01	0.75	0.01	105.0	26.0	40.3	23.9	12.40
217	July 11, 1993	28.9	17.8	46.8	4.98	4.87	0.22	80.5	131.6	50.4	20.8	2.83
218	July 11, 1993	33.9	11.8	31.4	2.46	0.81	0.04	153.2	31.4	42.5	19.6	51.51
219	July 11, 1993	88.4	22.9	48.0	4.02	0.29	0.03	279.5	90.1	53.5	24.1	157.30
220	July 11, 1993	58.6	31.0	63.2	3.21	0.64	0.04	264.8	147.5	56.8	19.5	1.10
221	July 11, 1993	87.5	23.4	48.3	4.02	0.29	0.05	273.4	100.3	55.4	23.7	164.78
222	July 11, 1993	82.6	43.7	63.8	2.38	0.50	0.61	278.3	128.4	90.0	22.8	0.62
223	July 12, 1993	35.6	17.7	24.6	2.36	0.61	0.00	205.0	32.2	19.4	*	0.02
224	July 12, 1993	83.4	18.4	24.8	1.83	0.16	0.00	251.4	66.8	28.8	*	2.66
225	July 13, 1993	73.8	10.1	23.7	1.94	0.06	0.00	231.9	34.1	32.0	22.2	1.22
226	July 13, 1993	97.7	20.4	39.0	3.31	0.18	0.18	259.9	99.9	46.1	22.3	22.65
227	July 14, 1993	98.9	19.8	34.9	2.55	0.05	0.01	288.0	81.0	35.7	23.1	66.55
228	July 14, 1993	61.8	11.6	18.2	1.57	0.13	0.02	173.9	59.4	22.4	17.9	9.43
229	July 14, 1993	99.5	19.6	35.6	2.50	0.03	0.00	299.0	78.7	38.0	22.9	61.33
230	July 14, 1993	59.8	10.2	21.1	1.47	0.08	0.01	174.5	45.7	26.5	18.5	1.47
231	July 14, 1993	33.1	6.6	22.2	1.36	0.87	0.16	106.8	23.5	35.5	17.6	4.67
232	July 15, 1993	54.7	8.6	24.3	1.68	0.15	0.01	183.1	31.7	35.5	18.4	2.35
233	July 15, 1993	92.1	21.1	43.4	3.69	0.03	0.00	300.8	93.0	48.8	24.1	117.83
234	July 15, 1993	71.3	12.5	28.8	1.99	0.00	0.00	207.5	64.3	34.4	18.2	0.40
235	July 15, 1993	89.4	20.6	43.5	3.62	0.03	0.00	299.6	99.6	46.0	23.7	124.14
236	July 15, 1993	70.9	14.4	29.4	2.18	0.02	0.01	202.6	64.5	40.5	17.8	1.70
237	July 18, 1993	45.8	23.6	48.1	2.55	0.41	0.21	202.0	73.3	57.8	36.4	0.96
238	July 18, 1993	20.1	21.1	34.3	5.07	0.19	0.00	57.4	82.9	62.7	43.8	0.00
239	July 18, 1993	85.4	67.2	68.9	6.13	0.14	0.04	108.6	114.8	82.0	18.9	0.88

Table 1. (continued)

Sample Number	Date Collected	Ca, mg L ⁻¹	Mg, mg L ⁻¹	Na, mg L ⁻¹	K, mg L ⁻¹	Fe, mg L ⁻¹	Mn, mg L ⁻¹	HCO ₃ , mg L ⁻¹	SO ₄ , mg L ⁻¹	Cl, mg L ⁻¹	SiO ₂ , mg L ⁻¹	Discharge, L s ⁻¹
240	July 18, 1993	95.4	23.6	49.8	4.11	0.05	0.02	292.3	89.1	55.2	24.5	128.05
242	July 18, 1993	62.7	35.8	65.5	4.73	0.02	0.01	184.9	254.3	50.7	20.4	0.45
245	July 21, 1993	91.6	9.5	22.0	1.30	0.08	0.00	239.8	54.2	22.4	*	0.65
246	July 21, 1993	102.1	23.4	23.9	1.50	0.08	0.00	289.2	76.2	35.5	*	0.03
247	July 21, 1993	86.8	13.7	22.7	1.02	0.03	0.00	243.5	66.1	22.6	26.8	1.25
248	July 21, 1993	51.1	9.5	15.2	1.02	0.12	0.03	158.0	40.7	17.3	*	0.09
112A	July 13, 1993	112.8	20.4	38.3	2.29	0.08	0.02	306.9	84.2	50.3	27.2	6.29
116A	July 13, 1993	114.9	23.7	41.8	2.73	0.14	0.17	350.3	83.6	46.9	30.2	6.46
117A	July 13, 1993	96.5	19.4	36.9	3.11	0.15	0.14	261.2	94.5	42.9	21.7	23.13
118A	July 13, 1993	84.0	13.9	32.9	1.98	0.02	0.00	202.0	74.9	46.4	17.8	6.46
119A	July 8, 1993	96.6	19.4	34.9	2.61	0.15	0.02	261.2	78.8	40.8	22.0	80.25
120A	July 8, 1993	106.2	25.0	44.4	3.96	0.31	0.06	322.2	111.5	43.6	27.4	34.04
121A	July 9, 1993	50.2	31.4	68.7	11.88	0.04	0.00	372.8	54.8	145.1	43.6	1.64
122A	July 9, 1993	96.3	20.7	38.6	3.27	0.20	0.03	286.8	91.5	41.9	23.2	96.16
127A	July 9, 1993	48.1	28.6	61.3	8.50	0.16	0.02	216.6	135.3	68.7	54.1	1.08
128A	July 9, 1993	65.6	39.1	52.4	8.79	0.23	0.10	245.9	195.7	51.7	51.6	1.61
129A	July 7, 1993	58.2	34.8	58.0	8.28	0.08	0.00	230.7	178.7	63.7	49.4	1.42
145A	July 14, 1993	111.2	24.1	34.6	2.94	0.00	0.00	343.5	87.9	31.7	26.8	16.45
146A	July 14, 1993	95.1	18.4	33.4	2.33	0.04	0.00	275.8	78.6	36.3	22.7	71.87
147A	July 8, 1993	52.6	30.2	58.6	11.62	0.07	0.01	318.5	136.1	38.2	49.7	1.50
148A	July 8, 1993	110.8	24.1	42.8	3.12	0.10	0.01	330.7	109.4	43.1	25.4	38.28
149A	July 8, 1993	92.3	23.0	48.3	3.98	0.05	0.03	295.3	92.7	56.6	24.8	116.84
150A	July 7, 1993	79.0	25.1	39.4	3.01	0.15	0.03	271.5	61.3	53.1	21.8	1.42
151A	July 7, 1993	93.7	21.9	42.7	3.87	0.12	0.01	280.1	89.1	47.3	24.0	188.42
157A	July 21, 1993	107.9	17.6	23.8	1.56	0.05	0.01	313.0	65.3	19.8	24.2	27.84
158A	July 15, 1993	52.4	19.3	31.8	2.72	0.00	0.00	252.0	44.0	28.8	24.7	6.20
159A	July 15, 1993	64.3	17.9	30.1	2.24	0.00	0.00	238.6	59.2	26.9	23.0	6.80

to secondary mineral precipitation, and Q_b is the loss of solutes via biologic uptake [Paces, 1986]. Because anthropogenic inputs appear to be minimal and the rates of secondary mineral precipitation and biologic uptake cannot be estimated with the available data, the flux equation was simplified to the following:

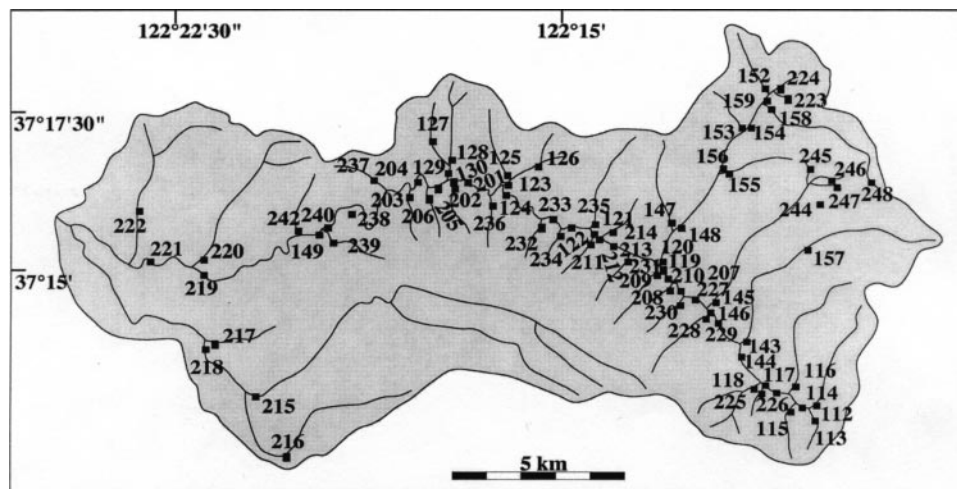
$$Q_r = Q_t - Q_w - Q_d - Q_g,$$

where Q_r is redefined to mean the net flux from bedrock weathering (flux released minus flux precipitated) and Q_t is redefined as the total flux less formation water contributions. Q_t was estimated conservatively by assuming that all Cl^- not deposited by the atmosphere is derived from formation water. Mean concentration of saline groundwater in the region [Johnson,

1980] was used as a reference to calculate, relative to Cl^- , the contribution of other major chemical constituents from formation water. Using this method, the contribution of formation water to the base flow signature ranged from 14 to 70% with a mean contribution of 28%. The relative contribution of formation water, as might be expected, is partly inversely correlated with mass flux per unit area ($R^2 = 0.16$).

To arrive at Q_g , the observed HCO_3^- concentration was multiplied by a gravimetric factor (0.4917) under the assumption that half of the HCO_3^- in solution is volatile and not derived from the weathering of rocks. This assumption generally gives a good approximation for the actual dissolved carbonate in calcium-bicarbonate waters [Hem, 1989].

Base flow chemical-weathering rates (mass/time/area) were calculated for each subcatchment using the adjusted stream chemistry

**Figure 3.** Locations of sample points in the Pescadero Creek watershed.

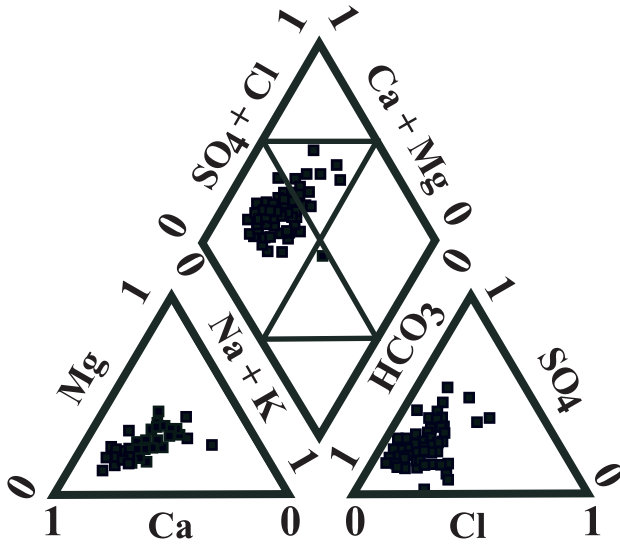


Figure 4. Trilinear diagram of base flow ionic constituents.

data, discharge data, and area data (Figure 8). The area of each subcatchment was determined by planimeter measurements on topographic maps. Base flow chemical denudation rates (length/time) were then determined by dividing the subcatchment weathering rates by an assumed bedrock density of 2.7 g cm^{-3} . The calculated rates range from 0.0004 to 0.02 mm yr^{-1} with high rates generally found in the eastern, high-elevation portion of the basin. High mass flux and chemical denudation that appear in other regions in the watershed may be at least partly controlled by faulting.

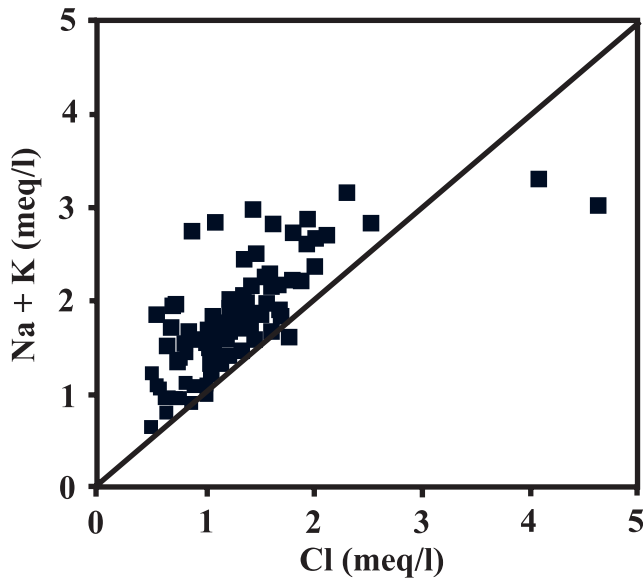


Figure 5. Plot of base flow samples showing the offset from the 1:1 stoichiometric relationship expected for the contribution of saline inputs.

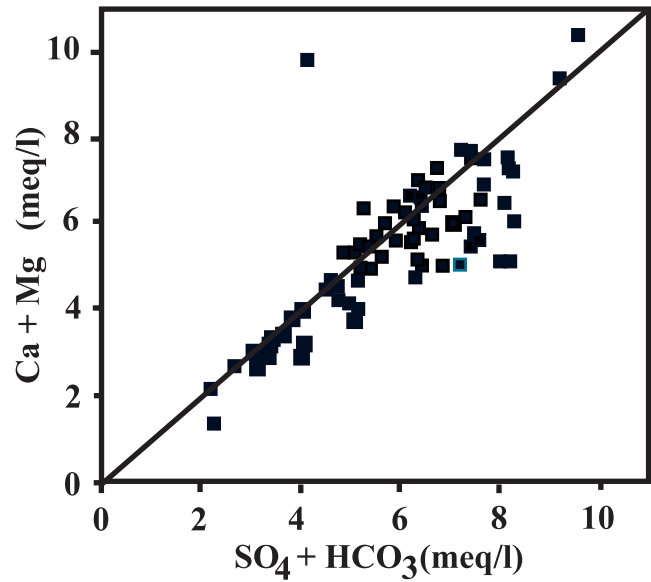


Figure 6. Plot of base flow samples showing the 1:1 stoichiometric balance between the products of weathering reactions involving carbonate and sulfide minerals.

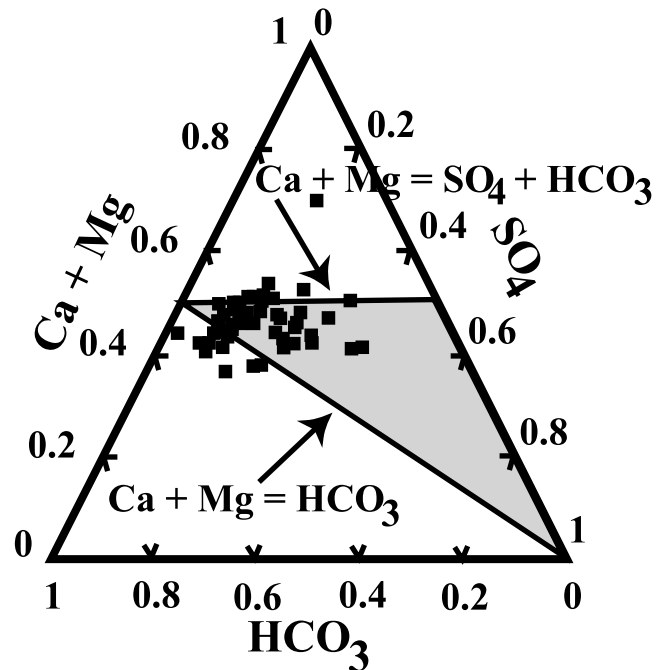


Figure 7. Ternary plot of carbonate and sulfate ionic constituents in base flow samples. Shaded region defines samples dominated by carbonate and sulfide weathering.

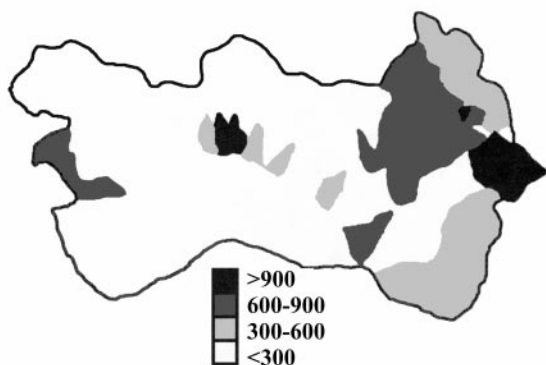


Figure 8. Net mass fluxes ($\text{mg s}^{-1} \text{km}^{-2}$) from the Pescadero Creek watershed under base flow conditions. Formation water contributions not included.

Using historical data collected at the USGS gauging station [Steele, 1968] and the same procedure as above, temporal chemical denudation rates (length/time) were calculated for the watershed. Values range from 0.0006 to 0.6 mm yr^{-1} . The total mean annual chemical denudation rate, determined from the stream composition at the mean annual discharge of 1134 L s^{-1} [Limneros *et al.*, 1979], is $\sim 0.03 \text{ mm yr}^{-1}$. The base flow component of the chemical denudation rate, computed from the mean base flow discharge of 100 L s^{-1} [Rojstaczer and Wolf, 1994], is 0.004 mm yr^{-1} . Figure 9 shows each solute as the fraction of total solutes (meq of x /total meq) across the discharge range.

5. Discussion

5.1. Sources of Solutes

Spatial trends in base flow chemical signature roughly correspond to three geologically distinct regions of the watershed [Steele, 1968]. Solute concentrations are typically highest in tributaries draining the Purisima Formation in the northcentral and northwestern portion of the basin (Figure 2), typically lowest in tributaries draining the Butano Sandstone in the southern part of the basin, and intermediate in tributaries draining the geologically complex northeastern portion of the basin. The distribution of Ca^{2+} and HCO_3^- is somewhat different, however, as the concentrations of these ions tend to decrease away from the northeastern part of the basin.

The oxidation of sedimentary pyrite appears to play a major role in the chemical signature of base flow. Pyrite is ubiquitous in the sedimentary units of the basin and is especially abundant in the organic mudstones of the Monterey Formation in the northeastern part of the basin [Clark, 1981].

Figures 4 and 7 suggest that the congruent dissolution of calcite and dolomite is the dominant chemical-weathering process producing the chemical character of base flow. This process may be driven by sulfuric acid formed from the oxidation of pyrite. Like pyrite, carbonate sources are found throughout the system, especially in the northeastern part of the basin, where the Mindego Basalt, the Lambert Shale, and the Monterey Formation contain abundant sources of calcium carbonate as dolomite, calcareous cement, and carbonate fossils and concretions [Steele, 1968]. The tributaries in the northeastern part of the watershed contain the highest Ca^{2+} and HCO_3^- concentrations and tend to be supersaturated with respect to calcite and dolomite. Because these tributaries contribute a large percentage

of the discharge to Pescadero Creek, Pescadero Creek also carries an elevated Ca^{2+} and HCO_3^- signal and remains supersaturated with respect to calcite and dolomite throughout its course, as the low-discharge tributaries downstream do not dilute the signal significantly.

The oxidation of pyrite may be the dominant source of SO_4^{2-} to base flow (Baldwin, 1967a). However, $\text{Na}^+ - \text{SO}_4^{2-}$ formation waters are also present in the basin (Johnson, 1980) and likely contribute significant amounts of SO_4^{2-} to the system. Elevated SO_4^{2-} concentrations are observed in tributaries draining the intensely-fractured Purisima Formation, where groundwaters appear to be flushing these formation waters to the surface (Steele, 1968).

Along with SO_4^{2-} , concentrations of Na^+ , Cl^- , Mg^{2+} , K^+ , and SiO_2 are also highest in tributaries draining the Purisima Formation. Again, contributions by formation waters are likely responsible for the enhanced signals, though significant fractions of SiO_2 and Na^+ almost certainly result from the weathering of abundant silicic and andesitic volcanic debris in the unit [Clark, 1981]. Tributaries draining the Purisima are at or very near equilibrium with amor-

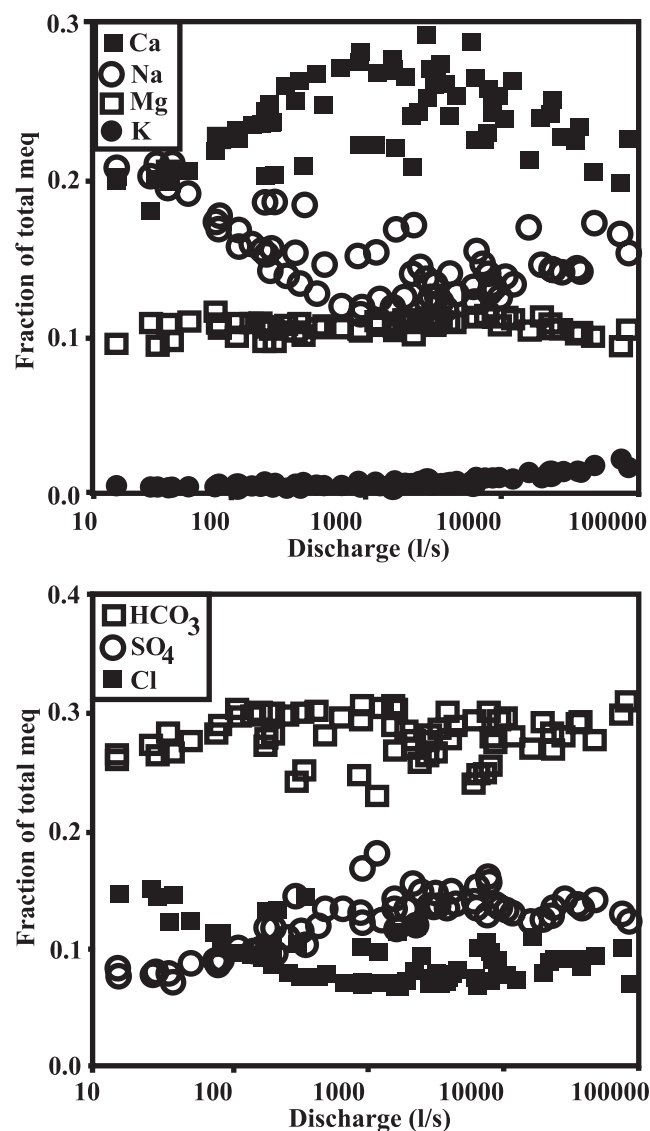


Figure 9. Variation in the chemical composition of Pescadero Creek as a function of discharge (data from Steele [1968]).

phous SiO₂, perhaps owing to the dissolution of the silicic glass debris, and may receive significant amounts of both SiO₂ and Na⁺ from the weathering of Na-plagioclase in the andesitic debris.

It is difficult, given the uncertainties and complexity in the local mineralogy, to assess the dominant secondary mineral products resulting from silicate weathering. Montmorillonite is one possible significant weathering product. The formation of montmorillonite requires either volcanic glass or ferromagnesian minerals as the source material [Berner, 1971], and both are found throughout the Pescadero basin. Volcanic glass is abundant in the Purisima Formation, where montmorillonoid coatings are also found on sandstone grains [Lerbekmo, 1957]. Ferromagnesian minerals commonly outcrop in the eastern part of the watershed in the form of the Mindego Basalt or as pillow basalt flows in the Vaqueros Sandstone [Clark, 1981]. Weathering of these minerals also appears to contribute a significant portion of the Mg²⁺ signal to basin waters [Baldwin, 1967a]. If montmorillonite is the dominant secondary mineral product, the bulk of silicate weathering appears to involve volcanic rocks rather than the more stable detrital feldspar grains found in the arkosic sandstones of the watershed.

5.2. Chemical Weathering and Rates of Denudation

Investigations by Mast *et al.* [1990] and Williams *et al.* [1993] have used stoichiometric mass balance models similar to that of Garrels and Mackenzie [1967] to determine the amount of dissolved material contributed by each mineral as a result of the chemical-weathering process. Unfortunately, the model requires prior knowledge of the weathered mineral compositions and cannot be properly used if unknown sources of solutes are present in the system. Thus, in the Pescadero Creek watershed, the complex lithology and the presence of formation waters of highly variable composition preclude the use of the model.

However, the chemical and discharge data do provide considerable information about chemical-weathering processes and denudation. In the Pescadero Creek watershed the bulk of the base flow chemical signature appears to be contributed by the oxidation of pyrite and the dissolution of carbonates. This observation is not surprising given that the rate of calcite dissolution is 6 orders of magnitude greater than the rate of aluminosilicate dissolution under neutral pH conditions [Plummer *et al.*, 1979; Lasaga, 1984] and that pyrite is even less resistant to weathering than calcite [Berner and Berner, 1987]. Because these ubiquitous minerals readily dissolve or oxidize, spatial rates of chemical denudation are strongly correlated with variability in recharge rather than lithology. As a result, chemical denudation rates tend to be greatest in the eastern part of the watershed where the orographic enhancement of rainfall yields the highest rates of recharge and discharge per unit area. Temporal rates of chemical denudation are also strongly correlated with discharge in the Pescadero Creek watershed. Historical data show that the concentration of total ions varies only by a factor of 4 over a discharge range of 4 orders of magnitude, further exemplifying the dissolution of highly soluble minerals as the major source of solutes.

Pescadero Creek undergoes a distinct change in overall composition at a discharge of $\sim 100 \text{ L s}^{-1}$ (Figure 9). Beyond this discharge, Ca²⁺ replaces Na⁺ as the dominant cation, and SO₄²⁻ replaces Cl⁻ as the second most abundant anion. The other ions retain the same relative abundance throughout the discharge range. As a function of total ionic concentration, Na⁺ and Cl⁻ concentrations decrease exponentially ($R^2 = 0.978$ and 0.952 , respectively), Ca²⁺ and SO₄²⁻ concentrations decrease logarithmically ($R^2 = 0.960$ and 0.882 , respectively), and Mg²⁺ and HCO₃⁻ concentrations decrease linearly ($R^2 = 0.985$ and 0.980 , respectively).

The observed chemical behavior of Pescadero Creek likely results from the leaching of soil solutions by shallow flow cells

and surface runoff during high-discharge events. In the Mattole River basin, Kennedy [1977] found that Na⁺ is leached from surface soils much more rapidly than Ca²⁺ and Mg²⁺. This observation explains the rapid decrease in Na⁺ concentration relative to the concentrations of Ca²⁺ and Mg²⁺ in the Pescadero basin. Similarly, Cl⁻ shows relatively little absorption in soils [Kennedy, 1977], explaining its rapid decrease in concentration in the Pescadero basin relative to SO₄²⁻ and HCO₃⁻. SO₄²⁻ tends to accumulate in the soil zone because it is more strongly adsorbed than Cl⁻ and is also produced in significant amounts by the decomposition of organic matter [Kennedy, 1977]. The slow dilution of SO₄²⁻ in the Pescadero basin relative to the other solutes is probably attributable to such a reservoir of SO₄²⁻. Evidence for the influence of water–bedrock interactions [Anderson *et al.*, 1997] in the water chemistry/discharge magnitude relationships is lacking.

6. Conclusions

Base flow chemical signals were used to determine the weathering reactions that control the groundwater chemistry of a geologically heterogeneous, mountainous watershed. Additionally, chemical and discharge data were used to calculate spatial and temporal rates of chemical denudation in the watershed. Major ion signatures appear to result from cyclic salt and formation water inputs and from the weathering of highly soluble or easily oxidized minerals, such as pyrite, calcite, and dolomite. If montmorillonite is the dominant secondary mineral product, then the bulk of silicate weathering in the watershed probably involves volcanic rocks. Because highly soluble and easily oxidized minerals contribute the bulk of the chemical signal to basin waters, spatial and temporal rates of chemical denudation are constrained largely by recharge rather than local variations in lithology.

At the subcatchment scale, base flow chemical denudation rates range from 0.0004 to 0.02 mm yr⁻¹ and tend to be greatest in the eastern part of the watershed where the orographic enhancement of rainfall yields the highest rates of recharge and discharge per unit area. Including the influence of seasonal precipitation on the watershed, mean annual chemical denudation rates are found to be $\sim 0.03 \text{ mm yr}^{-1}$. This mean value is a factor of 2 greater than the 0.013 mm yr⁻¹ value calculated for the Pacific slopes region of the United States, which includes both the coastal ranges and Sierra Nevadas of California [Judson and Ritter, 1964]. The discrepancy between the values likely arises because the minerals in marine units of the coastal ranges weather much more readily than the granitic rocks of the Sierra Nevadas. However, both of these rates are very similar to rates found in watersheds of the Himalayas and Tibetan Plateau (0.013–0.027 mm yr⁻¹) and greater than rates found in watersheds of the Andes (0.009–0.011 mm yr⁻¹) [Summerfield and Hulton, 1994]. Thus the chemical denudation rate of the Pescadero Creek watershed is comparable to the rates of some of the world's most rapidly weathering areas. While the basin is undergoing comparatively modest uplift, its lithology and climate make it highly susceptible to chemical weathering.

Acknowledgments. We thank Paul Baker for helpful suggestions and the use of laboratory materials and William Schlesinger and Emily Klein for the use of laboratory equipment. We also thank the rangers at Memorial Park and Skyline Open Space Preserve for their cooperation and assistance with data collection. Funding for this research was provided by NSF EAR-9458376 and EAR-9119082.

References

- Akers, J. P., and L. E. Jackson, Jr., Geology and ground water in western Santa Cruz County, California, with particular emphasis on the Santa Margarita sandstone, *U.S. Geol. Surv. Water Resour. Invest.*, 77–15, 7 pp., 1977.

- Anderson, R. S., and K. M. Menking, The Quaternary marine terraces of Santa Cruz, California: Evidence for coseismic uplift on two faults, *Geol. Soc. Am. Bull.*, 106, 649–664, 1994.
- Anderson, S., W. E. Dietrich, R. Torres, and D. R. Montgomery, Concentration-discharge relationships in runoff from a steep, channeled catchment, *Water Resour. Res.*, 33, 211–225, 1997.
- Baldwin, A. D., Geologic and geographic controls upon the rate of solute erosion from selected coastal river basins between Half Moon Bay and Davenport, California, Ph.D. dissertation, Stanford Univ., Stanford, Calif., 1967a.
- Baldwin, A. D., Geologic and geographic controls upon the rate of solute removal from selected coastal river basins between Half Moon Bay and Davenport, California, in *American Water Resources Conference, 3rd Annual, San Francisco, CA, Proc. Ser. 3*, pp. 548–562, Am. Water Resour. Assoc., Middleburg, Va., 1967b.
- Berner, E. K., and R. A. Berner, *The Global Water Cycle: Geochemistry and Environment*, Prentice-Hall, Englewood Cliffs, N. J., 1987.
- Berner, R. A., *Principles of Chemical Sedimentology*, McGraw Hill, New York, 1971.
- Brabb, E. E., Geologic map of Santa Cruz County, California, *U.S. Geol. Surv. Misc. Invest. Map 1-1905*, 1989.
- Brabb, E. E., and E. H. Pampeyan, Geologic map of San Mateo County, California, *U. S. Geol. Surv. Map 1257A*, 1983.
- California Department of Water Resources, Coastal San Mateo County Investigation, *Bull. Calif. Dept. Water Resour.*, 138, 322 pp., 1966.
- Clark, J. C., Stratigraphy, paleontology, and geology of the Central Santa Cruz Mountains, California Coast Ranges, *U.S. Geol. Surv. Prof. Pap.*, 1168, 1981.
- Cummings, J. C., et al., Geology of the northern Santa Cruz Mountains, California, *Bull. Calif. Div. Mines Geol.*, 181, 179–220, 1962.
- Garrels, R. M., and F. T. Mackenzie, Origin of the chemical compositions of some springs and lakes, in *Equilibrium Concepts in Natural Water Systems, Adv. Chem. Ser.*, vol. 67, edited by R.F. Gould, pp. 222–242, Am. Chem. Soc., Washington, D.C., 1967.
- Gieskes, J. M., and W. C. Rogers, Alkalinity determination in interstitial waters of marine sediments, *J. Sediment. Petrol.*, 43, 272–277, 1973.
- Hem, J. D., Study and interpretation of the chemical characteristics of natural water, 3rd ed., *U.S. Geol. Surv. Water Supply Pap.*, 2254, 263 pp., 1989.
- Johnson, M. J., Geology and groundwater in north-central Santa Cruz County, California, *U.S. Geol. Surv. Water Resour. Invest.*, 80–26, 33 pp., 1980.
- Judson, S., and D. F. Ritter, Rates of regional denudation in the United States, *J. Geophys. Res.*, 69, 3395–3401, 1964.
- Kennedy, V. C., Geochemistry of the Mattole River of Northern California, *U.S. Geol. Surv. Open File Rep.*, 78–205, 324 pp., 1977.
- Knops, J. M. H., The influence of epiphytic lichens on the nutrient cycling of an oak woodland, Ph.D. dissertation, Arizona State Univ., Tempe, 1994.
- Lasaga, A. C., Chemical kinetics of water-rock interactions, *J. Geophys. Res.*, 89, 4009–4025, 1984.
- Lerbekmo, J. F., Authigenic montmorillonoid cement in andesitic sandstones of central California, *J. Sediment. Petrol.*, 27, 298–305, 1957.
- Limneros, J. T., et al., Water resources data for California, vol. 2, *U.S. Geol. Surv. Water Data Rep.*, CA-79-2, 509 pp., 1979.
- Mast, M. A., J. I. Drever, and J. Baron, Chemical weathering in the Loch Vale watershed, Rocky Mountain National Park, Colorado, *Water Resources Res.*, 26, 2971–2978, 1990.
- Moore, T. L., and T. M. Worsley, Orogenic enhancement of weathering and continental ice-sheet initiation, *Spec. Pap. Geol. Soc. Am.*, 288, 75–89, 1994.
- Nilsen, T. H., and E. E. Brabb, Geology of the Santa Cruz Mountains, California, in *GSA Cordilleran Section Field Trip Guidebook*, 97 pp., Geol. Soc. of Am., Boulder, Colo., 1979.
- Paces, T., Rates of weathering and erosion derived from mass balance in small drainage basins, in *Rates of Chemical Weathering of Rocks and Minerals I*, edited by S.M. Colman, and D.P. Dethier, pp. 531–550, Academic Press, San Diego, Calif., 1986.
- Plummer, L. N., T. M. L. Wigley, and D. L. Parkhurst, Critical review of the kinetics of calcite dissolution and precipitation, in *Chemical Modeling in Aqueous Systems, Syp. Ser.*, vol. 93, edited by E.A. Jenne, pp. 537–573, Am. Chem. Soc., Washington, D.C., 1979.
- Rojstaczer, S., and S. Wolf, Hydrologic changes associated with the earthquake in the San Lorenzo and Pescadero drainage basins, *U.S. Geol. Surv. Prof. Pap.*, 1551E, E51–E64, 1994.
- Stallard, R. F., and J. M. Edmond, Geochemistry of the Amazon, 2, The influence of geology and weathering environment on dissolved load, *J. Geophys. Res.*, 88, 9671–9688, 1983.
- Steele, T. D., Seasonal variations in chemical quality of surface water in the Pescadero Creek watershed, San Mateo County, California, Ph.D. dissertation, Stanford Univ., Stanford, Calif., 1968.
- Summerfield, M. A., and N. J. Hulton, Natural controls of fluvial denudation rates in major world drainage basins, *J. Geophys. Res.*, 99, 13,871–13,883, 1994.
- Volk, T., Cooling in the late Cenozoic, *Nature*, 361, 123–124, 1993.
- Williams, M. W., A. D. Brown, and J. M. Melack, Geochemical and hydrologic controls on the composition of surface water in a high-elevation basin, Sierra Nevada, California, *Limnol. Oceanogr.*, 38, 775–797, 1993.

R. D. Phillips and S. Rojstaczer, Division of Earth and Ocean Sciences and Center for Hydrologic Science, Duke University, Box 90230, 106 Old Chemistry, Durham, NC 27708. (stuart@duke.edu)

(Received June 11, 1999; revised April 12, 2000; accepted April 20, 2000.)